Computer-Assisted Interventions on liver: Feasibility of the "anchor needle" technique for real-time targeting of lesions with respiratory motion.

Ivan Bricault [1,2], Simon DiMaio [2], Olivier Clatz [3], Sonia Pujol [2,4], Kirby Vosburgh [4], Ron Kikinis [2]

[1] Laboratoire TIMC-IMAG-GMCAO, Institut d'Ingénierie de l'Information de Santé, Faculté de Médecine, 38706 La Tronche cedex (France) Ivan.Bricault@imag.fr

[2] Surgical Planning Laboratory, Radiology department, Brigham and Women's Hospital, Boston (USA)

[3] Projet Epidaure, INRIA, Sophia-Antipolis (France) [4] CIMIT/Harvard Medical School, Boston (USA)

INTRODUCTION

Computer-assisted navigation systems are now more and more widely used in clinical practice for interventional radiology and minimally invasive surgical procedures. They may involve robotic [1], optical [2] or electro-magnetic [3] devices in order to provide guidance to the physician. Many liver procedures can benefit from these computer-assisted navigation systems. Accurate placement of needles within the liver is a crucial part of diagnostic procedures such as tumor biopsies [4], or of advanced therapeutic procedures such as radiofrequency tumor ablations [5]. Contrary to other anatomical regions that do not move during intervention (e.g., skull or spine), liver moves significantly with respiration [6]. Since computer-assisted liver interventions are generally too complex to be performed during a single apnea, the ability to continuously monitor the position of a liver target during several respiration cycles is a critical challenge. A few systems can benefit from real-time imaging (ultrasound, fluoroscopy, interventional MRI) for a direct monitoring of target position. However, most systems can use only preoperative imaging like CT and conventional MRI, subsequently relying on a precise registration of preoperative planning and imaging data into the intraoperative situs. In the case of moving organs such as liver, a continuous registration would be a complex and computationally demanding task.

The "anchor needle" technique is presented here, as a first approximate approach to liver motion monitoring compatible with real-time constraints. The "anchor needle" is a fine needle with its tip percutaneously placed inside the liver, and its outside base tracked in real-time with 6 degrees of freedom: in particular, it is possible to equip the needle base with a miniaturized magnetic sensor such as a 1.8mm-diameter microBIRD^{TM} coil (Ascension technology, Burlington, VT, USA). In this study, we will investigate the conditions under which the liver motion can be adequately estimated from the magnetically tracked "anchor needle"

motion. This analysis will be based on computerized tomography (CT) data acquired during animal experiments. In addition, computer simulations will use a simplified liver and needle model and will illustrate various experimental conditions.

MATERIAL AND METHOD

The expected relationships between liver and anchor needle base and tip motions during respiration were investigated theoretically using specific computer simulation software. We simulated liver and needle deformations with a two-dimensional linear elastostatic material model, discretised using the finite element method [7]. We studied a simplified respiratory cycle, where liver was given a cranio-caudal translation while the needle experienced a rotational motion about a pivot point in the abdominal wall. The liver parenchyma was approximated as a homogeneous soft tissue rectangular area; border conditions allowed free deformations for the anterior and inferior edges, whereas the superior and posterior edges were constrained by the cranio-caudal translation motion, simulating a close relationship to the diaphragm (Fig. 1a). Several parameters were varied during computer simulations, in order to reproduce various experimental conditions: magnitude of cranio-caudal translation (*t*: 15mm—25mm), needle depth into the liver (*d*: 25mm—45mm), needle stiffness (*s*: 1%—100%), and abdominal wall stiffness around the needle rotational pivot point (*k*: 10%—70%).

Feasibility of the "anchor needle" technique was evaluated in vivo on 2 different pigs. A fine needle (22G) was placed percutaneously, under ultrasound guidance, in the liver of the pigs under general anesthesia. Two contrast-enhanced CT scans of the pig liver were then acquired on a Siemens 16 channel MDCT (collimation=1.5mm, slice thickness=2mm, reconstruction interval=1.5mm): one during an apnea at end-expiration (CT_{exp}), and the other during an apnea at end-inspiration (CT_{insp}). In the first pig, these CT acquisitions were performed twice with the needle in an intermediate (depth *d*=20mm) and a superficial (*d*=10mm) location. In the second pig, in addition, we created 2 synthetic tumors by introducing percutaneously, under ultrasound guidance and general anesthesia, 0.7 ml of silicon in the right and left liver lobe parenchyma before the CT acquisitions [8].

The "anchor needle" tip positions $I_{\exp}$ and I_{insp} were measured on both CT data CT_{exp} and CT_{insp}, respectively. The "anchor needle registration" $\vec{R}$ was then defined as the needle tip translation between end-expiration and end-inspiration $R = I_{insp} - I_{\exp}$ (Fig. 1). The translation $\vec{R}$ was applied to liver CT data CT_{exp} in order to compensate for the respiratory motion: $CT_{exp \rightarrow insp} = CT_{exp} + \vec{R}$. The accuracy of this "anchor needle registration" was evaluated by comparing the translated data $CT_{exp \rightarrow insp}$ with the data acquired at end-inspiration CT_{insp}. For this comparison, we computed a non-rigid registration between $CT_{exp \rightarrow insp}$ and CT_{insp} using the robust algorithm described in [9]. The resulting deformation field provided, for every point in the liver, a value of the "anchor needle" registration error.

RESULTS

The fine needle used for the animal experiments (22G) proved to be stiff enough so that its tip motion could be considered as rigidly related to the needle base motion (Fig.2).

The first pig demonstrated a large respiratory liver motion with a mean magnitude equal to 18.5mm (Fig. 3). The "anchor needle registration" could reduce the difference between inspiration and expiration to a mean magnitude of 7.4mm. The registration error was less than 5mm for 10% of the liver parenchyma, and less than 3mm for only 0.7% of the liver parenchyma. An additional translation applied to expiration data could improve the results obtained with the "anchor needle registration", reducing the mean error to 5.2mm. After this additional translation, the registration error was less than 5mm for 62% of the liver parenchyma, and less than 3mm for 29% of the liver parenchyma.

Computer simulations also demonstrated that, in some situations, the "anchor needle registration" would be improved by an additional translation (Fig. 4). Computer simulations showed that the magnitude of this additional translation would increase with an increasing cranio-caudal translation magnitude t or pivot point stiffness k, or with a decreasing needle depth d. The second experiment with pig #1, using a needle depth of d=10mm (instead of d=20mm for the first experiment) confirmed an increased registration error equal to 10.1mm (instead of 7.4mm).

The second pig demonstrated a smaller respiratory liver motion with a mean magnitude of 4.7mm (Fig. 5). Before the "anchor needle registration", the difference between inspiration and expiration was less than 5mm for 50.9% of the liver parenchyma, and less than 3mm for 12.3% of the liver parenchyma. The "anchor needle registration" reduced the difference between inspiration and expiration to a mean magnitude of 2.8mm. The registration error was then less than 5mm for 93.4% of the liver parenchyma, and less than 3mm for 57.2% of the liver parenchyma. Without any registration, the two liver tumors targeted during inspiration would be missed during expiration. On the contrary, the "anchor needle registration" allowed a correct targeting during both respiratory positions.

DISCUSSION

A 22G fine needle is commonly used for interventional radiology procedures. Since its diameter is very small, it gives to the procedure a desirable minimally invasive feature. Besides, it is observed here that a 22G anchor needle is rigid enough (Fig. 2), so that a magnetic sensor can be attached to its base and can reliably track the tip position. An alternative would be to use a needle where the magnetic sensor is directly inserted at the needle tip. Yet such a needle, for instance the 19G MagTrax needle (Traxtal®), would be larger and more invasive.

Computer simulations (Fig. 4) and pig #1 data (Fig. 3) show some limitations of the "anchor needle" technique. The accuracy decreases when the respiration translation range is large, when the needle is superficial or when the pivot point stiffness is increased. In

these situations, the liver presents some large local deformations in the neighborhood of the needle tip, and the anchor needle motion does not reflect adequately the global liver motion. As demonstrated by the need of an additional translation (Figs. 3-4), the magnitude of the anchor needle tip motion is smaller than the magnitude of the global liver motion. These extreme situations highlight the benefit of a quiet respiration, a deep anchor needle and a sub- (rather than inter-) costal position of the needle, associated with a decreased abdominal wall stiffness.

The case of pig #2 meets these requirements and shows that the "anchor needle registration" can help a computer-assisted intervention system to target a tumor in the presence of respiratory motion. Whereas only complex non-rigid registration algorithms would be able to exactly correct for liver motion and deformation during respiration, the "anchor needle" technique is a simple method whose results are compatible with clinical applications. For improved accuracy, this technique may also be used as an initialization step for a more sophisticated registration process. Since the "anchor needle registration" only requires the tracking of the outside base of a needle, it gives this approach a desirable real-time capability.

As a part of ongoing research, we are integrating the anchor needle technique into a computer-assisted liver intervention system that is currently under development [10]. This will allow us to add a new respiratory tracking functionality to the system, and to further evaluate the accuracy of the anchor needle technique.

This project was supported in part by a study grant from the French Radiological Society.

BIBLIOGRAPHY

[1] BOCTOR EM, TAYLOR RH, FICHTINGER G, CHOTI MA. *Robotically assisted intraoperative ultrasound with application to ablative therapy of liver cancer.* In: Visualization, Image-Guided Procedures, and Display; Galloway RL, Ed, Proceedings of SPIE vol. 5029, 2003.

[2] HERLINE AJ, HERRING JL, STEFANSIC JD, CHAPMAN WC, GALLOWAY RL, DAWANT BM. *Surface registration for use in interactive, image-guided liver surgery.* Comp Aid Surg 2000; 5:11-17.

[3] CLEARY K, BANOVAC F, LEVY E, TANAKA D. *Development of a liver respiratory motion simulator to investigate magnetic tracking for abdominal interventions.* In: Medical Imaging; Proceedings of SPIE vol. 4681 pp 25-29, 2002.

[4] HOWARD MH, NELSON RC, PAULSON EK, KLIEWER MA, SHEAFOR DH. *An electronic device for needle placement during sonographically guided percutaneous intervention.* Radiology 2001; 218:905-911.

[5] MCGHANA JP, DODD GD. *Radiofrequency ablation of the liver: current status.* AJR Am J Roentgenol 2001; 176:3-16.

[6] CLIFFORD MA, BANOVAC F, LEVY E, CLEARY K. *Assessment of hepatic motion secondary to respiration !for computer assisted interventions.* Comp Aid Surg 2002; 7:291-299.

[7] DIMAIO SP, SALCUDEAN SE. *Needle insertion modeling and simulation.* IEEE International Conference on Robotics and Automation 2002; pp. 2098-2105.

[8] RESTREPO JI, STOCCHI L, NELSON H, YOUNG-FADOK TM, LARSON DR, ILSTRUP DM. *Laparoscopic ultrasonography: a training model.* Dis Colon Rectum. 2001; 44:632–637.

[9] CLATZ O, DELINGETTE H, TALOS IF, GOLBY AJ, AYACHE N, KIKINIS R, JOLESZ FA, WARFIELD SK. *Robust Nonrigid Registration to Capture Brain Shift from Intra-Operative MRI.* IEEE trans. Med. Imaging, 2004. Submitted.

[10] VOSBURGH KG, STYLOPOULOS N, PUJOL S, SAN JOSE ESTEPAR R, KRISSIAN K, BRICAULT I, ELLSMERE J. *Guiding Abdominal Surgery with Image Registered Laparoscopic Ultrasound (IRLUS).* In: RSNA 2004, Radiological Society of North America, Chicago; November 2004.

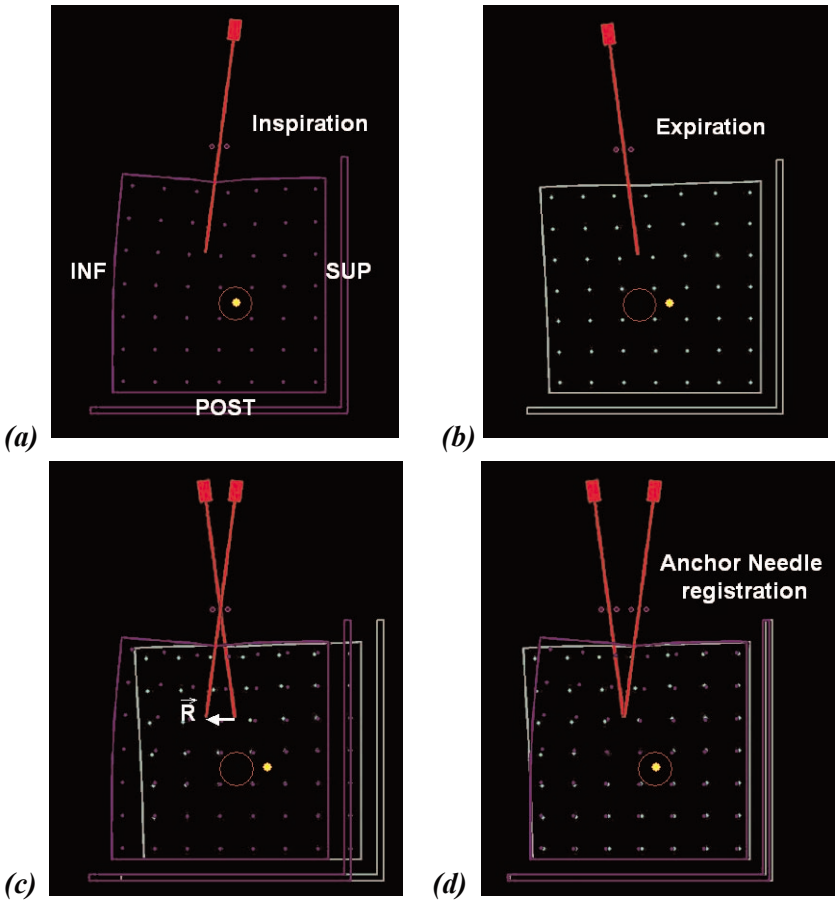

Figure 1. Principle of the "anchor needle registration".

(a-b) Simulation of liver motion and deformation during respiration. The liver (square area) is represented in supine position in this lateral view. The location of the diaphragm is shown close to the superior and posterior sides of the liver. A rigid anchor needle is here deeply inserted into the liver parenchyma (parameters used for these computer simulations: needle depth d=45mm, needle stiffness s=100%). At end-inspiration and end-expiration, the needle rotation about a pivot point in the abdominal wall is shown (pivot point stiffness k=10%). During respiration, the cranio-caudal translation magnitude of the liver has been set to t=15mm.

A tumor is represented in the liver parenchyma (yellow dot). If we assume that the position of this tumor has been targeted by a computer-assisted intervention system during inspiration (red circle, Fig. 1a), it is observed that the tumor would be missed during expiration (Fig. 1b).

(c) Combination of inspiration and expiration views. The "anchor needle" translation vector $R = I'_{insp} - I'_{\exp}$ *is represented.*

(d) Expiration data have been translated according to $\vec{R}$*, as demonstrated by the alignment between needle tip positions (*$I'_{\exp}$ *and* I'_{insp}*). This "anchor needle" registration has almost completely cancelled the respiratory motion. The tumor can now be adequately targeted during both inspiration expiration.*

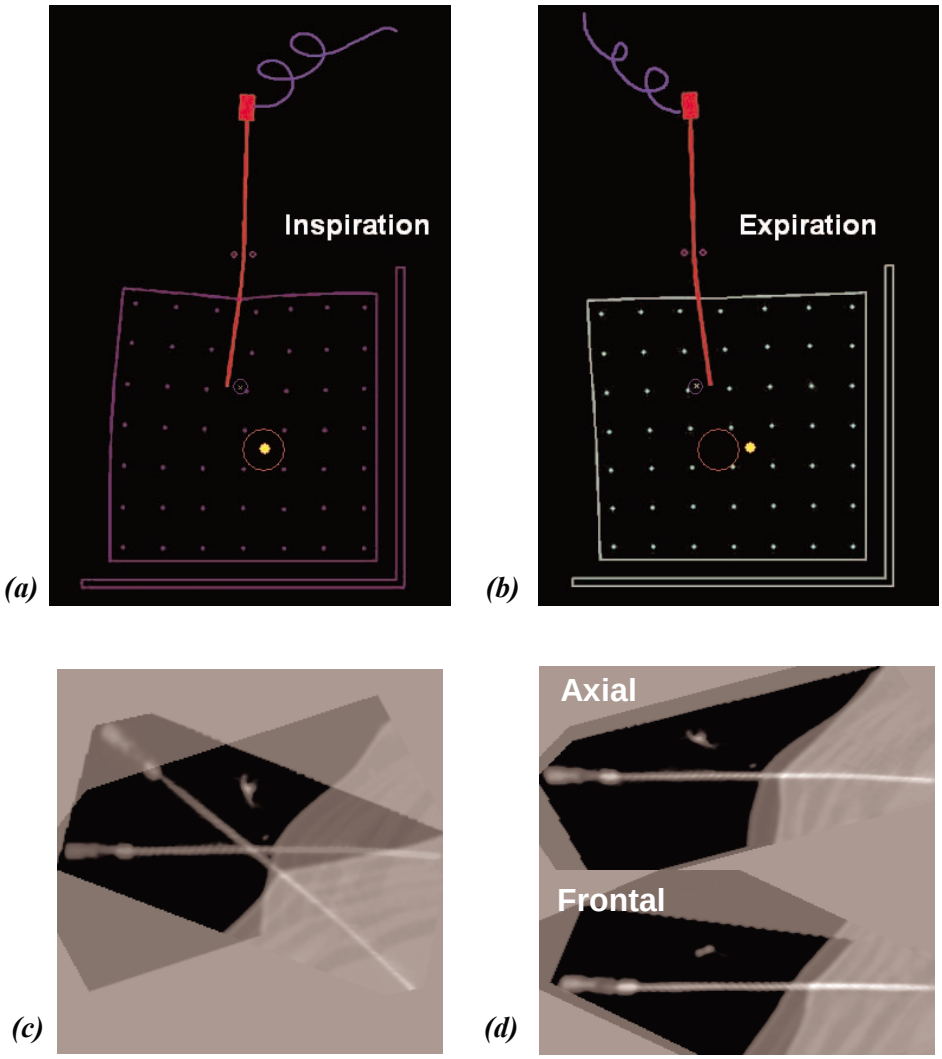

Figure 2. Effect of "anchor needle" stiffness

(a-b) Simulation of flexible needle deformations during respiration: same parameters as Fig. 1, except for needle stiffness (s=1% instead of 100%). A magnetic sensor is supposed to be attached to the needle base. Since the needle is not rigid, the position of the tip deduced from the magnetic sensor data (small blue circle) does not match the actual tip position. Thus a needle base tracking would not allow a correct estimation of the respiratory motion of the needle tip and liver tumor.

(c) Combination of experimental data of a 22G needle acquired at end-expiration and end-inspiration. The rotation of the needle during respiration is demonstrated.

(d) Same needle views during expiration and inspiration, after a rigid registration of both positions, shown in 2 orthogonal projections (axial and frontal). The needle during expiration is now almost perfectly aligned with the needle during inspiration. This demonstrates that a 22G needle experiences a rigid motion during respiration, with no detectable deformation between expiration and inspiration.

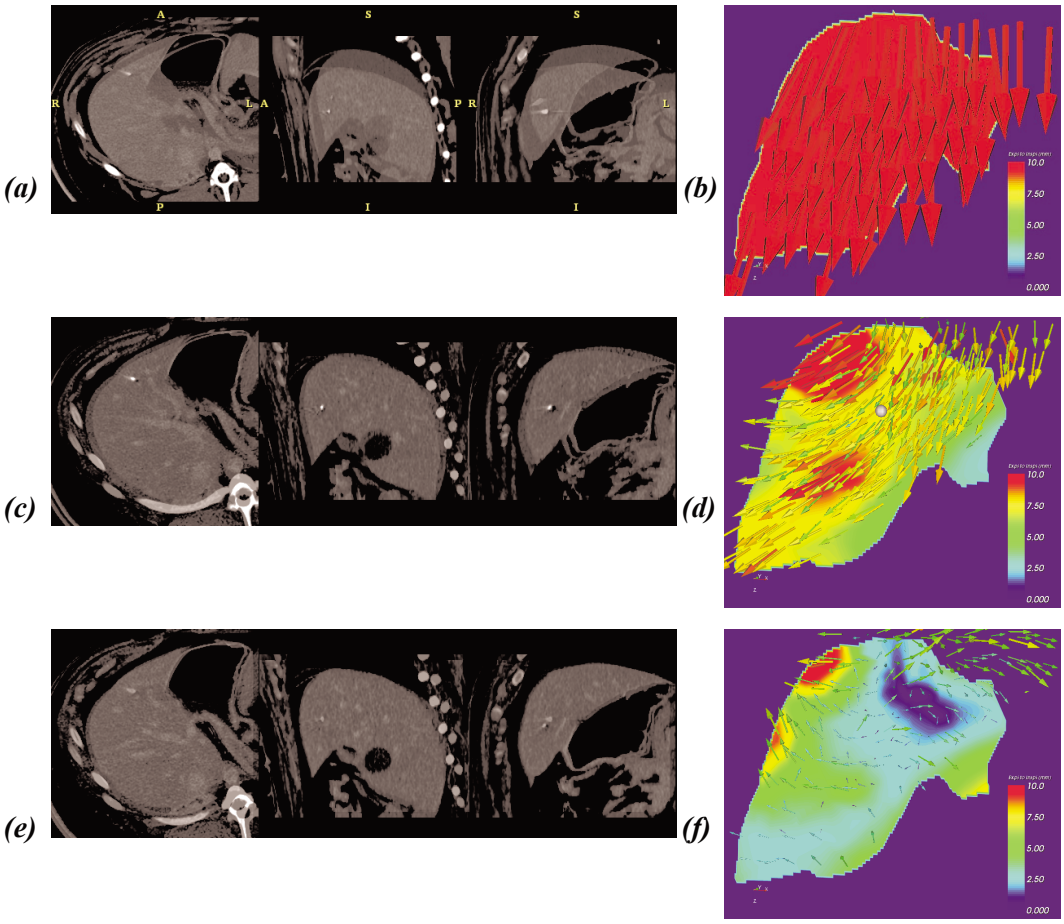

Figure 3. Experimental results, pig #1, needle depth d=20mm

(a) Combination of CT views at end-inspiration and end-expiration (axial, sagittal and frontal planes). The inferior and anterior motion of the liver between expiration and inspiration is well demonstrated in the sagittal view.

(b) 3D view of the liver motion field during inspiration (arrows). A frontal slice of the liver is also shown. The red color indicates that the motion magnitude is greater than 10mm (cf. color scale). The mean magnitude of liver respiratory motion in this pig is equal to 18.5mm.

(c-d) After the "anchor needle registration", combined inspiration and expiration views demonstrate a better alignment, but a mean error equal to 7.4 mm remains. The white sphere in Fig. 3d represents the position of the "anchor needle" tip.

(e-f) An additional translation applied to expiration data achieves a better registration, with a mean error now reduced to 5.2mm. Note that the motion field in Fig. 3f is now largely inhomogeneous, and represents complex liver deformations during respiration that can not be corrected by a simple rigid registration.

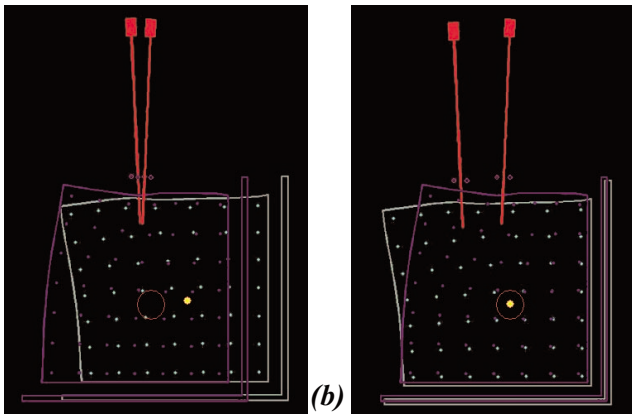

Figure 4. Simulations with a large translation (t=25mm), a superficial needle (depth d=25mm) and a stiff pivot point (k=70%) ***(a)*** ***(b)***

(a) Combination of expiration and inspiration views after the "anchor needle registration". In this extreme situation, there are large liver deformations around the needle, and the needle tip does not follow the global liver respiratory motion. Here, the "anchor needle registration" does not allow a correct targeting of the tumor.
(b) Combination of expiration and inspiration views after applying an additional translation on the expiration view. Now both views are globally approximately registered, whereas the needle tips and the highly deformed liver in the neighborhood are not aligned.

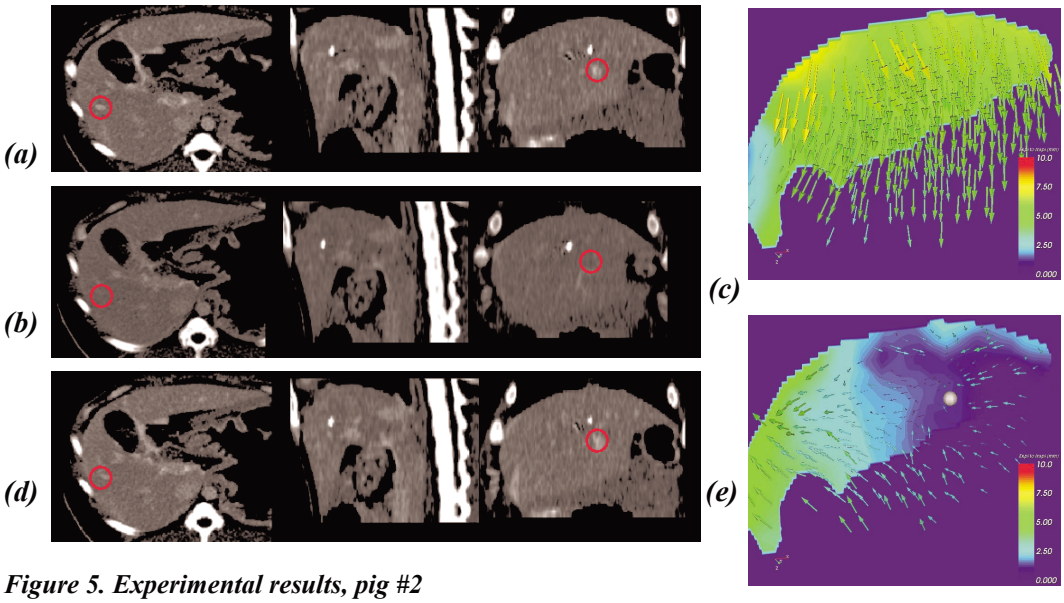

Figure 5. Experimental results, pig #2
(a) Axial, sagittal and frontal CT views at end-inspiration. Two tumors (red circles) are targeted.
(b) CT views at end-expiration. Due to liver respiratory motion, the tumors targeted during inspiration would be missed during expiration. (c) The motion field demonstrates the liver inferior and anterior motion during inspiration, with a mean magnitude equal to 4.7mm.
(d-e) After the "anchor needle registration", both tumors stay in the targeted area at end-expiration. The mean difference between inspiration and expiration has been reduced to 2.8mm.